ELSEVIER

Polymer 42 (2001) 2413–2426

polymer

www.elsevier.nl/locate/polymer

Permeability of N_2, Ar, He, O_2 and CO_2 through biaxially oriented polyester films — dependence on free volume

E.-A. McGonigle[a], J.J. Liggat[a,*], R.A. Pethrick[a], S.D. Jenkins[b], J.H. Daly[a], D. Hayward[a]

[a]*Department of Pure and Applied Chemistry, University of Strathclyde, 295 Cathedral Street, Glasgow G1 1XL, UK*
[b]*Du Pont Polyester, Wilton Research Centre, Middlesbrough TS90 8JE, UK*

Received 15 December 1999; received in revised form 8 July 2000; accepted 8 August 2000

Abstract

Permeability, diffusion and solubility coefficients are reported for biaxially orientated polyester films based on poly(ethylene terephthalate) [PET], poly(ethylene naphthalate) [PEN] and copolymers containing PET and PEN moieties. Data for cast amorphous sheets and materials produced with different biaxial draw ratios are compared. The crystallinity of the samples was assessed using differential scanning calorimetry and density measurements. The changes in the void structure at a molecular level were investigated using positron annihilation lifetime spectroscopy (PALS). The variation of the gas diffusion behaviour with the gas used (carbon dioxide, nitrogen, argon, helium and oxygen) reflects the effects of change in morphology on the solubility and diffusivity components of the permeability. The diffusivity of the gas is influenced not only by both the changes in the void size and content at a molecular level, but also by the effects of crystallinity on the percolation behaviour of the gas through the matrix. Changes in the extent of chain alignment also have a profound affect on the solubility of the gas in the matrix. The observed behaviour for the gas permeation can be interpreted as being the result of the complex interplay of changes in the crystalline content, the polymer chain alignment and the void structure of the amorphous phase.

Keywords: Poly(ethylene terephthalate); Poly(ethylene naphthalate); Copolymers

1. Introduction

1.1. Orientation

Drawing or stretching of an amorphous polymer film is known to lead to reorientation and closer chain packing, and restriction of chain mobility [1]. Since sorption and diffusion may be assumed to occur in the amorphous regions, these processes can be altered due to changes in the spatial distribution of the amorphous phase during drawing. At present there are simple models which describe the gas permeability in biaxially oriented semi-crystalline polymers such as poly(ethylene terephthalate) (PET). Early works by Michaels and Brixler [2] revealed that sorption and diffusion take place exclusively through the amorphous phase. It is accepted that the stretching process can break up the initial structure of the polymer and transform it into a new structure [3–6]. Any areas of crystallinity — resulting from the stretching process — either lengthen the diffusion pathway or reduce the amorphous chain mobility. Other mechanisms proposed are associated with lengthening of crystallites or tautening of tie molecules in the structure. All these changes will increase the tortuousity of the pathway for a permeant molecule.

When polymers such as PET are stretched, substantial improvements in gas barrier properties are obtained due to changes in shape, extent and perfection of the non-permeable crystalline regions as well as a result of the ordering effects imparted in the amorphous regions. During the orientation process the chains become aligned in the direction of the applied stress, whilst the aromatic rings and crystal planes are thought to become parallel with the film surface [3–5]. Stretching in a second direction then redistributes the structure toward the new direction of stress, and a balanced structure with the aromatic rings and crystal planes almost parallel to the two orthogonal stretch directions is obtained. Obviously, this will be a function of the fabrication variables used. The chain alignment increases the tautness or rigidity, and decreases the mobility within the remaining amorphous regions of the polymer [6]. Indeed, uniaxial orientation in PET has been found to decrease the diffusion rate of CO_2 through a combination of an increased tautness

* Corresponding author. Tel.: +44-141-548-4351; fax: +44-141-548-4822.
E-mail address: j.j.liggat@strath.ac.uk (J.J. Liggat).

0032-3861/01/$ - see front matter
PII: S0032-3861(00)00615-7

of the chains and a decrease in the mobility of the oriented segments, coupled with an increase in the tortuousity of the diffusion pathway [7]. Biaxial orientation causes a further decrease by constraining the amorphous chain segments, which bridge between the more ordered regions. One would expect that increasing the orientation would improve the barrier properties; but this need not be the case if fibrillation occurs.

Poly(ethylene naphthalate) (PEN), is a semi-crystalline polymer akin to PET. Its unique properties lie in its higher melt viscosity and polymorphism [8]. With PEN, uniaxial stretching produces a highly localised alignment of naphthalene planes parallel to the surface of the film [9–11]. Biaxially oriented PEN shows bimodal orientation of the chain axes in the draw directions [9]. The net effect of the stretching process is to constrain the surrounding amorphous regions and/or lengthen the diffusion pathway. Necking is a common problem when orienting (uniaxial or biaxial) PEN films and high draw areas have to be employed to produce films of uniform thickness. Therefore, it has been found necessary in practice to incorporate a second component in the polymer, such as poly(ether imide), that will disrupt the co-operative alignment of naphthalene groups parallel to the surface [9,10]. For the PETN copolymer systems studied in this paper it may be envisaged that at certain compositions the effect of the co-monomer is to disrupt the alignment of aromatic planes.

The microstructures of PET and PEN are relatively well defined and two distinctive conformers exist in completely amorphous samples: *gauche* and *trans* ethylene glycol moieties. Stretching of the PET or PEN causes an alignment of molecules in the stretch direction, with individual segments becoming extended (*gauche* to *trans*) [12]. This is generally accompanied by an increase in crystallinity, an increase in rigidity of the intervening amorphous phase and a decrease in gas permeability. Upon stretching, one would perhaps expect to see a reduction in the free volume due to closer chain packing and restricted mobility in the amorphous regions [1].

1.2. Gas permeability

The model commonly used to describe the permeation process of a gas through a polymer film is the solution-diffusion model [7,13]. This model assumes that the permeation of a gas through a polymer film occurs in three stages; first, sorption of the gas into the polymer; second, diffusion of the gas through the bulk polymer; and third, desorption from the opposite face of the film. Permeability, P, can thus be defined as a combination of the diffusivity, D, of the gas dissolved in the polymer, and the gas solubility, K:

$$P = DK \tag{1}$$

At a molecular level it is important to understand the effect that polymer chain packing has on the free volume and free volume distribution, since physical, mechanical and transport properties are sensitive to the amount of free volume available [14].

The molecular free volume is defined as the difference between the total volume and the volume occupied by the polymer molecules. Free volume theories assume that both the mobility of a polymer segment and movement of a diffusing species are determined by the amount of free volume in the system. The diffusing molecule can only move from one place to another when the local free volume exceeds a critical value [7,13].

Light and Seymour [15] looked at the gas transport properties of copolyesters based on PET and poly(1,4-cyclohexamethylene terephthalate) and concluded that modifications which restricted local molecular motions in the β-relaxation region in turn decreased the permeability to oxygen and carbon dioxide. Similar explanations have been proposed by Weinkauf and Paul [16] for thermotropic liquid-crystalline copolyesters, and by Kim et al. [17] in a study encompassing gas transport properties and dynamic mechanical properties of blends and random copolymers of bisphenol-A polycarbonate and tetramethyl-bisphenol-A polycarbonate. The incorporation of naphthalate in the structure of PET will effectively diminish the local chain motions associated with the β-relaxation [18].

1.3. Positron annihilation lifetime spectroscopy and free volume

Gas diffusion coefficients have been successfully fitted to the following equation predicted by the free volume theory [13,19,20]:

$$D = A \exp\left(\frac{-B}{V_F}\right) \tag{2}$$

where A and B are constants for a given gas. A is related to the size and shape of the permeant and B is related to the minimum hole size of the polymer matrix required for a diffusional jump. A drawback of this free volume approach is that the permeant is assumed to be approximately spherical and its interactions with the matrix purely van der Waals.

There have been numerous studies of the possible correlation between positron annihilation and gas transport [19,21–27]. In polymers, PALS gives rise to a long-lived component, which is a consequence of *ortho*-positronium (*o*-Ps) annihilation in amorphous regions. The *o*-Ps species localises itself in free volume cavities of radius 0.2–0.6 nm, a range which correlates to the non-bonded interatomic distances in polymers, and the molecular radii of diffusing substances [26]. Analysis of the PALS data is usually carried out in terms of three lifetime components in polymers: τ_1 which is attributed to *para*-positronium (*p*-Ps) annihilation; τ_2 which is attributed to free positron and positron-molecular species annihilation; and τ_3 which is attributed to *o*-Ps annihilation. In molecular systems the

Table 1
Details of the melt cast polymer films used

Material	Mol% PEN	M_w	M_n	IV (dl/g)	T_g (°C)	Density (g cm^{-3})
PET	0	106,000	37,400	0.809	81	1.3352
PETN8	8	100,000	35,700	0.780	85	1.3343
PETN16	16	97,100	38,100	0.819	89	1.3336
PETN84	84	73,900	29,000	0.839	119	1.3276
PEN	100	69,300	28,700	0.836	124	1.3267
BLEND	[a]	81,600	31,700	0.780	100	1.3323

[a] BLEND is PETN3/PETN95 [50/50 wt%].

o-Ps localised in a cavity annihilates through an exchange process with an electron of opposite spin from molecules forming the cavity wall. Each lifetime has a corresponding intensity (I) relating to the number of annihilations occurring at a particular lifetime. The long lifetime component is the important quantity for polymers (τ_3, I_3). The free volume cavity size is related to τ_3. It follows that PALS can provide valuable information on both mean size and relative number of free volume cavities probed by *o*-Ps.

The average free volume size (V_F) for spherical cavities can be calculated [28–30]:

$$V_F = \frac{4\pi R^3}{3} \tag{3}$$

where the cavity radius, R is calculated from the *o*-Ps lifetime results:

$$\tau_3 = \frac{1}{2}\left[1 - R(R + \Delta R) + \left(\frac{1}{2\pi}\right)\sin(2\pi R/(R + \Delta R))\right]^{-1} \tag{4}$$

where, ΔR represents an electron layer thickness and is estimated as 0.166 nm by fitting τ_3 to known vacancy sizes of molecular crystals. Eq. (4) can be used to calculate R from experimentally measured values of τ_3.

Furthermore, the fractional free volume, f, can be found from the empirical equation:

$$f = CV_F I_3 \tag{5}$$

where, V_F is in nm^3, I_3 in %, and C is an arbitrarily chosen scaling factor for a spherical cavity and is typically assigned [26] a value of 1.5.

Successful correlations of gas diffusivity and permeability with free volume measured using PALS have been obtained for polyimides [19], PEEK [21,24], epoxies [22,23] and polycarbonates [25,27]. Hill et al. [26] studied the effect of copolymer composition on free volume and related the results to gas permeability in PET/PCT copolyesters. It was found that increasing the concentration of PCT in the polyester copolymer series increased the gas permeability and free volume. The PALS results were subjected to the semi-empirical equations (3) and (5) to calculate V_F and f. These results were found to follow the Cohen–Turnbull theory [31] which is defined below:

$$D = C\exp\left(\frac{-\gamma v^*}{f}\right) \tag{6}$$

where, C and γ are constants, v^* the critical free volume cavity size necessary for diffusive displacements. The best fit to the Cohen–Turnbull theory was provided by $\tau_3^3 I_3$. The study showed the usefulness of PALS for relating free volume and transport properties. Similarly, Tanaka et al. [19] found a clear correlation between log D and V_F calculated from Eq. (3).

In this paper we report gas transport measurements for a series of biaxially oriented PET, PEN and PETN copolymers. The effects of orientation on the gas transport parameters are discussed with reference to crystallinity, chain orientation and free volume. The role of segmental mobility will be discussed in a subsequent paper [32].

2. Experimental

2.1. Materials

Cast amorphous sheets approximately 230 μm thick-provided by ICI Polyester (Table 1), were cut into 6 cm squares and stretched on a T. M. Long Stretcher at the Wilton Research Centre. Operation of the film stretcher is based on the movement of two bars at right angles to each other using hydraulically driven rods [33]. Samples were drawn simultaneously in the machine direction (MD) and transverse direction (TD) above T_g using a draw rate of 425% s^{-1}. Two draw areas were obtained for each film as shown in Table 2; aspect ratios are also tabulated. Density measurements were performed at 25°C using a density column containing solutions of toluene and Arklone [1,1,2-trichloro-1,2,2-trifluoroethane]. It should be noted that a commercial grade of PET (Laser +) was used throughout this study.

2.2. Differential scanning calorimetry and density measurements

Temperature scans were performed on the biaxially

Table 2
Conditions used for stretching and properties of the oriented films

Material	Draw temperature (°C)	Draw area[a]	Aspect ratio[a]
PET	107	6.8	1.41
		12.8	1.43
PETN8	106	6.8	1.41
		12.2	1.45
PETN16	117	7.0	1.45
		13.6	1.42
PETN84	139	10.5	1.44
		12.0	1.33
PEN	145	8.4	1.46
		12.2	1.45
BLEND	120	10.1	1.50
	128	14.7	1.44

[a] Draw area = (machine direction ratio) × (transverse direction ratio); aspect ratio = (machine direction ratio)/(transverse direction ratio).

oriented films from 30 to 300°C, at a rate of 10°C min^{-1} and a sensitivity of 10 mcal, using a Perkin–Elmer DSC2 calorimeter controlled by a BBC Master microcomputer with software developed at the University of Birmingham by Dr Jim Hay. Indium was used to calibrate the instrument, and all scans were performed under nitrogen at a flow rate of 60 ml min^{-1}. All scans were performed in triplicate. The glass transition temperature was defined as the temperature at which the change in heat capacity was one half its maximum value [34]. Melting and crystallisation temperatures were defined using the peak maximum value.

2.3. Gas permeability measurements

Gas permeabilities were obtained using a constant volume apparatus. The volumes of the downstream and upstream chambers were taken as 200 cm^3. Throughout the measurement, the upstream pressure remained virtually constant due to low fluxes and was measured using a high-pressure transducer (750B MiniBaratron). The downstream pressure was monitored using a low-pressure transducer (10 Torr MKS Baratron).

The polymer sample was a circular disk of 7 cm diameter. The thickness was measured on 50 points of the film using a Mitutoyo digital micrometer with a resolution of 1 μm. Data for both the original cast amorphous films and biaxially oriented films are presented for the permeability study. The polymer film was held between the two halves of the stainless steel cell with two flat *o*-rings thus ensuring a good seal between the membrane and the gas cell. The sample was then de-gassed for 36 h and a leak-rate measured on the downstream side. Leak-rates of 5 mTorr h^{-1} or below were acceptable. A gas pressure was then introduced in the upstream side and the steady state permeation rate determined by recording the downstream transducer pressure readings at intervals suitable to the gas/polymer/pressure combination of interest. The upstream driving pressures were 4 atm for CO_2 and N_2, 3 atm for Ar and 2 atm for He.

Steady-state fluxes were obtained from pressure–time curves at times greater than three to four times the time-lag, θ [35]. Calculations of pressure rise due to permeation were carried out using a Mathcad™ 6.0 program based on Eq. (7).

$$P = Jl/A\phi_p \tag{7}$$

where, l is the membrane thickness, A is the membrane area and ϕ_p the pressure difference across the membrane. The flux, J is defined:

$$J = [dp/dt][V/T] \tag{8}$$

where dp/dt is the rate of change of pressure in the downstream volume, V, as a function of time and T is the temperature. Effective diffusion coefficients, D, were estimated using the film thickness, l, and the time-lag, θ, in the following relationship [13]:

$$\theta = \frac{l^2}{6D} \tag{9}$$

The effective solubility coefficients were then estimated using Eq. (1). Reproducibility for identical film samples was found to be ±3–4% for the permeability coefficient, ±8–9% for the diffusion coefficient and ±10–12% for the solubility coefficient.

A MOCON Oxtran 10/50A oxygen permeability tester was used to measure the oxygen permeabilities of the films at 30°C. A film, 10 × 10 cm^2 was placed between the two halves of the permeability chamber and the rig was flushed with nitrogen at a flow rate of approximately 10 ml min^{-1} to completely remove traces of oxygen. The following day, the apparent oxygen transmission rate under nitrogen was measured to give information on the background count due to leaks in the system. This was performed in duplicate to give a background value in $cm^3\ m^{-2}\ day^{-1}$. The gas flow in the upper half of the cell was then switched over to oxygen and the sample left to equilibrate overnight. This was followed by measurement of the oxygen transmission rate as the oxygen emerging from the opposite face is carried away by the carrier gas to a sensor. Again measurements were conducted in duplicate. The penetrants used in this study had purities of at least 99%.

2.4. PALS measurements

The positron annihilation measurements were determined using a conventional fast–fast coincidence system which has been detailed previously [36]. The positron source was $^{22}NaCl$ sandwiched between Kapton foil. Sample films (15 × 15 mm^2 and 20 to 40 μm thick) were carefully stacked together to make samples of approximately 5 mm thickness. Two equivalent stacks, held together with PTFE tape, were then sandwiched around the source with a copper backing to provide a copper–sample–source–sample–copper sandwich. The

Table 3
Thermal properties and densities of the biaxially oriented films

Sample	Draw area	T_m (°C)	ΔH_m (kJ kg^{-1})	X_{DSC} (%, w/w)	Density (g cm^{-3})	X_ρ (%, v/v)
PET	6.8	250 ± 1	37 ± 4	31	1.3652	25.2
PET	12.8	251 ± 2	38 ± 2	32	1.3628	23.2
PETN8	6.8	245 ± 1	35 ± 1		1.3593	20.2
PETN8	12.2	244 ± 1	33 ± 4		1.3556	17.1
PETN16	7.0	229 ± 1	31 ± 3		1.3577	18.9
PETN16	13.6	229 ± 1	29 ± 1		1.3596	20.5
PETN84	10.5	251 ± 2	31 ± 1		1.3470	10.0
PETN84	12.0	250 ± 1	31 ± 1		1.3478	10.6
PEN	8.4	277 ± 1	45 ± 2	43	1.3452	8.5
PEN	12.2	278 ± 1	50 ± 1	48	1.3421	5.9
BLEND	10.1	241 ± 2	26 ± 1		1.3465	9.6
BLEND	14.7	241 ± 2	28 ± 2		1.3441	7.6

copper lifetime is accounted for in τ_1 and does not affect the analysis. The PAL measurements were made using two BaF_2 scintillators coupled to fast photomultipliers mounted in-line on an Oxford Instruments DC-2 cryostat. Using a ^{60}Co source and the energy window set for ^{22}Na events, the timing resolution of the apparatus was determined to be 220 ps. Lifetime spectra were measured at 25°C for 6 h, giving approximately a million counts per spectrum. Runs were conducted in triplicate. The data was processed using the PATFIT [37] program which consists of RESOLUTION and POSITRONFIT fitting programs.

The RESOLUTION of the instrument was measured using a single crystal of benzophenone, which has a well-defined lifetime. The POSITRONFIT is a least squares program which fits both a lifetime (τ) and intensity (I) to each of the exponential making up the spectra. Three lifetimes were defined, but the long lifetime components (τ_3, I_3), characteristic of *o*-Ps annihilation, are the important parameters for polymers and amorphous materials. The free volume cavity size is related to τ_3 and the number of *o*-Ps annihilation sites related to I_3. The short lifetime component (τ_1) corresponding to *p*-Ps annihilation, was fixed at 0.125 ns and the intensities of I_3 and I_1 constrained at a ratio of 3:1.

3. Results

3.1. Differential scanning calorimetry and density measurements

The DSC and density results on the oriented films are presented in Table 3. The density measurements provided a measurement of the crystalline content of the films. An increase in density was observed on going from a cast amorphous film to a biaxially oriented film. The apparent degree of crystallinity (X_ρ), expressed as a volume fraction was calculated using the following

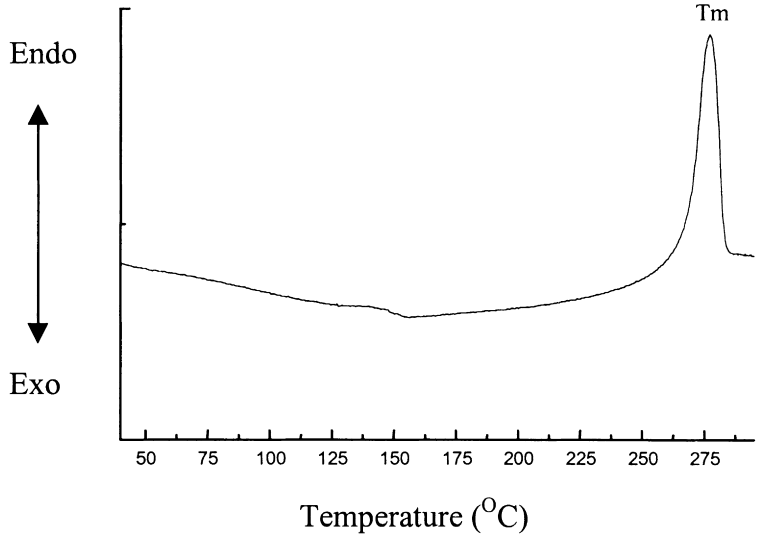

Fig. 1. Typical DSC scan for a biaxially oriented film.

relationship:

$$X_\rho = \frac{\rho - \rho_a}{\rho_c - \rho_a} \quad (10)$$

where, ρ is the density of the semi-crystalline sample, ρ_c is the density of the perfect polymer crystal and ρ_a the density of amorphous polymer. The values used for PET and PEN were ρ_a 1.3347 g cm^{-3} and 1.3267 g cm^{-3} and ρ_c 1.4534 g cm^{-3} and 1.4109 g cm^{-3}, respectively. The X_ρ values revealed significant changes in the samples upon orientation. Values of crystallinity could only be calculated for PET and PEN from the DSC (X_{DSC}) measurements since heat of fusion values for the fully crystalline polymer, ΔH_0, are available only for the homopolymers:

$$X_{DSC} = \frac{\Delta H_{exp}}{\Delta H_0} \quad (11)$$

where, ΔH_{exp} is the experimentally measured heat of fusion, and ΔH_0 for PET and PEN are quoted as 117.6 and 103.7 J g^{-1}, respectively [38,39]. A large discrepancy was noted in the crystallinity values calculated for PEN by the DSC and density techniques. The discrepancy is much larger than can be accounted for by the difference between mass-based crystallinity (DSC) and volume-based crystallinity (density). Similar discrepancies with PEN have been noted by other researchers [8], with DSC producing values of crystallinity up to 20% greater than those from density measurements. To rationalise the discrepancies it has been suggested that the literature value of ΔH_0 for PEN is too low. Another problem could lie with the DSC technique in the inaccurate estimation of baselines in the vicinity of the melting endotherms; however, this effect would not be as large as the observed discrepancy. Alternatively, the reliability of the density measurement could be questioned, as there is the distinct possibility that the amorphous phase may not have a uniform density after stretching [40].

Table 4
Helium permeability coefficients for the PET/PEN polyesters at 25°C (CA refers to the original cast amorphous sheet)

Material	Draw area	$P \times 10^{13}$ $\left(\frac{cm^3(STP)\ cm}{cm^2\ s\ cmHg}\right)$
PET	CA	3155
	6.8	1778
	12.8	1022
PETN8	CA	2979
	6.8	1625
	12.2	1120
PETN16	CA	3001
	7.0	1320
	13.6	1092
PETN84	CA	2504
	10.5	987
	12.0	675
PEN	CA	2115
	8.4	540
	12.2	508
BLEND	CA	2667
	10.1	1540
	14.7	1166

3.2. Gas transport properties

The transport coefficients (P, D and K) for the biaxially oriented polyester films are presented in Tables 4 and 5. The corresponding cast amorphous sheets data is included for He and CO_2 only. Thickness effects were a particular problem with CO_2 and the high naphthalate polymers (PETN84 and PEN). No permeability data could be obtained because the time for equilibration through these films was significant in relation to the measured leak-rate. The oxygen permeability coefficients obtained by Oxtran measurements are presented in Table 6.

The permeability coefficient defines the total volume of gas passing through the polymer film per second and was observed to increase in the order $N_2 < Ar < O_2 < CO_2 <$ He. Intuitively one would expect a gas like He to have greater access to parts of the polymer structure than say O_2 and this trend was not unexpected purely on the basis of the size of the permeant. The trend also reflects the condensability of the gas in the polymer with CO_2 being the most condensable.

Only permeability coefficients are tabulated for He transport owing to problems encountered in the accurate time-lag measurement technique for these thinner samples (Table 4). The problem stems from the fact that values of time-lag (θ) are reduced to a few seconds and cannot be determined with accuracy. Similar problems have been encountered by Holden and co-workers with linear low-density polyethylene [41].

A clear reduction in permeability (P) relative to the cast film value was observed for all of the oriented samples, and the higher draw area produced the lowest value. These effects were postulated to arise mainly from a decrease in segmental mobility of the chains as they are oriented. At the low draw areas, PEN and the PETN copolymers had lower permeabilities than PET. When stretched further, PETN8 and PETN16 exhibited a larger P relative to PET suggesting that the comonomers have disrupted the alignment of the chains.

With Ar and N_2, an increase in K and a decrease in D were observed on going from a low to a high draw area film. The exception to this rule was found to be the blend, where a decrease in K for both Ar and N_2 was observed with increasing draw area. For all draw areas the permeability coefficients showed a general decrease with incorporation of naphthalate. The magnitude of P appears to be dominated by the kinetic term (D) which is influenced by the presence of a bulkier or more rigid moiety. Indeed, a progressive reduction in D was observed as the naphthalate content

Table 5
Transport coefficients for the PET/PEN polyesters at 25°C (CA refers to the original cast amorphous sheet. / — data could not be obtained owing to the low fluxes obtained)

Material	Draw area	Gas	$P \times 10^{13}$ $\left(\frac{cm^3(STP)\ cm}{cm^2\ s\ cmHg}\right)$	$D \times 10^{10}$ $\left(\frac{cm^2}{s}\right)$	$K \times 10$ $\left(\frac{cm^3(STP)}{cm^2\ atm}\right)$
PET	6.8	Ar	16	7.5	167
	12.8		21	4.8	336
PETN8	6.8		25	7.9	238
	12.2		16	2.8	450
PETN16	7.0		18	6.9	202
	13.6		15	4.0	292
PETN84	10.5		6	1.1	193
	12.0		4	2.6	272
PEN	8.4		9	2.3	305
	12.2		2	0.7	219
BLEND	10.1		16	4.9	256
	14.7		12	4.9	179
PET	CA	CO_2	146	10.7	1039
	6.8		173	8.6	1534
	12.8		178	8.7	1550
PETN8	CA		129	10.9	899
	6.8		178	6.4	2120
	12.2		177	3.6	3724
PETN16	CA		71	5.6	968
	7.0		145	5.6	1974
	13.6		131	6.3	1587
PETN84	10.5		43	2.6	1255
	12.0		29	1.4	1627
PEN	8.4		22	1.0	1762
	12.2		18	0.6	2446
BLEND	CA		38	7.6	380
	10.1		96	9.6	1089
	14.7		93	8.0	886
PET	6.8	N_2	9	7.8	88
	12.8		7	2.7	194
PETN8	6.8		10	7.5	101
	12.2		7	2.3	101233
PETN16	7.0		5	4.1	84
	13.6		4	1.8	174
PETN84	10.5		/	/	/
	12.0		1.7	1.3	103
PEN	8.4		/	/	/
	12.2		1.7	1.0	120
BLEND	10.1		4.3	3.8	87
	14.7		1.9	2.5	59

increased, reflecting the presence of a more rigid structure in the matrix. Interestingly, PETN8 showed unusually high gas solubility and low diffusivity and a reduction of *P* relative to PET is only achieved for Ar and N_2 at the higher draw area. Orientation of the PETN3–PETN95 blend also acted to improve the gas transport properties with all the gases studied, due to the effect of alignment of the organised regions on the kinetic contribution.

The results for CO_2 transport were rather surprising. Firstly, increased values of *P* were measured relative to the corresponding cast film. Inspection of the data showed that this was the combined effect of a decrease in *D* due to reduced mobility and increased percolation pathlengths and, more interestingly, to an increase in the apparent solubility. This data implies increased polymer–penetrant interactions with CO_2, but contrasts with that of Brolly et al. where solubility decreased upon orientation, and diffusivity decreased for PEN but anomalously increased for PET [42].

The oxygen permeability coefficients for the drawn films were also consistent with the described trends, and revealed a reduction in *P* with increasing naphthalate contents. As with argon and nitrogen, compared with PET at the low draw area the PETN8 copolymer yielded a higher value of *P*, which decreased at the higher draw area suggesting an improved alignment/tautening of the naphthalate segments in the chain. As with all of the gas transport data, the reductions in *P* and *D* were more pronounced for the PETN84 and PEN polymers.

Table 6
Oxygen permeability coefficients for the PET/PEN polyesters at 30°C

Material	Draw area	$P \times 10^{13}$ $\left(\frac{cm^3(STP)\ cm}{cm^2\ s\ cmHg}\right)$
PET	6.8	36
	12.8	31
PETN8	6.8	35
	12.2	29
PETN16	7.0	30
	13.6	26
PETN84	10.5	8.7
	12.0	9.0
PEN	8.4	7.4
	12.2	7.5
BLEND	10.1	20
	14.7	20

3.3. PALS

Although the films used in positron annihilation work were relatively thin (20–40 μm), use of a multiple, sandwiched configuration allowed measurements to be made on the same sample used for the permeation measurements. Before commencing the experiments, it was necessary to check for surface layer effects. As with Tanaka et al. [19] in their work on polyimides, we found no substantial differences between thick and thin films other than those accountable to the morphological differences (Table 7). This method, therefore, can be assumed to yield PALS measurements, which may be directly correlated with the diffusion data.

The effects of biaxial orientation on the PALS data are not immediately clear, and do not allow for the possible changes of shape of the cavity structure. Stretching is known to substantially alter the spatial distribution and aggregation state of the amorphous component [1], which would presumably influence *o*-Ps pick-off. A similar situation has been observed with PALS experiments on PE fibres drawn from ratios 1–12, where the lifetime and intensity data were not sensitive to changes in chain conformations [43]. Large changes in conformation are known to occur in PE when drawn, but clearly, these do not have a large effect on the lifetime spectra. This suggests that *o*-Ps is formed between the lamellae and hence, the chain organisation that occurs in the crystalline regions is not being sensed [43].

The PALS results were reassessed paying particular attention to the possible morphological effects in these stretched systems. It was initially proposed by Hill and co-workers in a study relating free volume to gas permeability data for PET/PCT copolymers [26] that V_F (Eq. (3)), τ_3^3, $\tau_3^3 I_3$ and fractional free volume, f, in the Cohen–Turnbull equation (Eq. (6)) could be correlated with gas transport values. Parameters from the raw PALS data were calculated for the biaxially oriented films (Table 8). The trends are more clearly shown for the naphthalate systems in Figs. 2–5.

In addition to mean fractional free volume, the distribution of hole size may also affect gas diffusion. Different gas barrier performance can result if the same amount of free volume is distributed in larger rather than smaller holes [25]. It is possible to analyse the PALS data in terms of a distribution of free volume [22,23,25], but the derived distribution is sensitive to the precision of the measurement of the decay curves [43]. Instrumental limitations precluded the determination of free volume distribution in this instance.

4. Discussion

4.1. Differential scanning calorimetry and density measurements

The study of gas transport in polymer films requires an understanding of the polymer morphology of the films. Differential scanning calorimetry can be used to determine the transition temperatures and enthalpies of crystallisation and fusion of polymer films. Crystallinity plays an important role in barrier properties and chain organisation can determine the path and extent of diffusion. Crystallinity not only reduces permeability by reducing the free volume of the amorphous phase, but also increases the tortuousity of the diffusion path for the penetrant [13].

The absence of a crystallisation exotherm (see Fig. 1) implies that the films have developed, to a full extent, the degree of crystallisation dictated by the drawing conditions. The PETN copolymers and the blend had lower heats of fusion than either PEN or PET. This observation suggested that the chain alignment in these systems was not as efficient as in the homopolymers. Nevertheless, the

Table 7
Comparison of PALS data at 25°C for PET films of differing thicknesses and morphologies

Material	Average thickness (mm)	τ_3 (ns)	I_3 (%)	$\tau_3 I_3$ (ns %)
Injection moulded plaque[a]	3	1.66 ± 0.02	23.0 ± 0.3	38.2 ± 0.9
Melt cast film	0.229	1.59 ± 0.02	23.0 ± 0.2	36.6 ± 0.8
Biaxially oriented film	0.041	1.67 ± 0.01	19.8 ± 0.2	33.1 ± 0.5
Biaxially oriented film	0.022	1.59 ± 0.01	20.6 ± 0.2	32.8 ± 0.5

[a] Sample run at 30°C.

Table 8
Lifetime, intensity and simple spherical cavity model results for the cast amorphous and biaxially oriented films at 25°C (CA refers to the original cast amorphous sheet)

Sample	Draw area	τ_3 (ns)	I_3 (%)	R (nm)	V_F (nm^3)
Laser	CA	1.59 ± 0.02	23.0 ± 0.2	0.245 ± 0.02	0.062 ± 0.002
	6.8	1.67 ± 0.01	19.8 ± 0.2	0.253 ± 0.01	0.068 ± 0.001
	12.8	1.59 ± 0.01	20.6 ± 0.2	0.244 ± 0.02	0.061 ± 0.001
PETN8	CA	1.61 ± 0.02	23.3 ± 0.2	0.247 ± 0.02	0.063 ± 0.002
	6.8	1.70 ± 0.01	21.4 ± 0.2	0.256 ± 0.01	0.070 ± 0.001
	12.2	1.60 ± 0.01	22.8 ± 0.2	0.245 ± 0.01	0.062 ± 0.001
PETN16	CA	1.66 ± 0.02	22.8 ± 0.3	0.252 ± 0.02	0.067 ± 0.002
	7.0	1.68 ± 0.01	21.9 ± 0.2	0.254 ± 0.01	0.068 ± 0.001
	13.6	1.66 ± 0.02	21.6 ± 0.2	0.252 ± 0.02	0.067 ± 0.002
PETN84	CA	1.59 ± 0.02	22.6 ± 0.2	0.244 ± 0.03	0.061 ± 0.002
	10.5	1.60 ± 0.01	22.2 ± 0.2	0.246 ± 0.01	0.062 ± 0.002
	12.0	1.59 ± 0.01	22.1 ± 0.2	0.244 ± 0.01	0.061 ± 0.001
PEN	CA	1.56 ± 0.02	22.8 ± 0.2	0.241 ± 0.02	0.059 ± 0.002
	8.4	1.59 ± 0.01	22.3 ± 0.2	0.244 ± 0.01	0.061 ± 0.002
	12.2	1.57 ± 0.01	23.1 ± 0.2	0.243 ± 0.02	0.060 ± 0.002
BLEND	CA	1.67 ± 0.02	21.4 ± 0.3	0.253 ± 0.02	0.068 ± 0.002
	10.1	1.64 ± 0.01	21.8 ± 0.2	0.250 ± 0.01	0.066 ± 0.001
	14.7	1.64 ± 0.01	21.5 ± 0.2	0.249 ± 0.01	0.065 ± 0.001

stretching conditions appear to have incorporated crystallinity in all of the systems and was consistent with the observations of Lu and Windle [44] who found that PETN random copolymers could crystallise over the full composition range under hot drawing conditions, with the crystallinity attributed to synergistic interactions of the sequences of PET and PEN units.

Within experimental error, no differences in melt temperature or endotherm were observed in going from the lower draw area to the higher draw area. This was consistent with a study by Cakmak et al. [45] who looked at PET biaxially oriented using a selection of fabrication variables, including draw temperature and draw ratio. They found that the position of the melting endotherm did not change significantly with the fabrication variables, but that the shape of the endotherm did.

Above the T_g region, another transition, which was not very well defined, was observed. At fast drawing rates like those used in this study, not all of the *trans* isomer population becomes incorporated into the crystalline phase but some is retained in the amorphous phase. Lee and Sung [47] also observed this transition

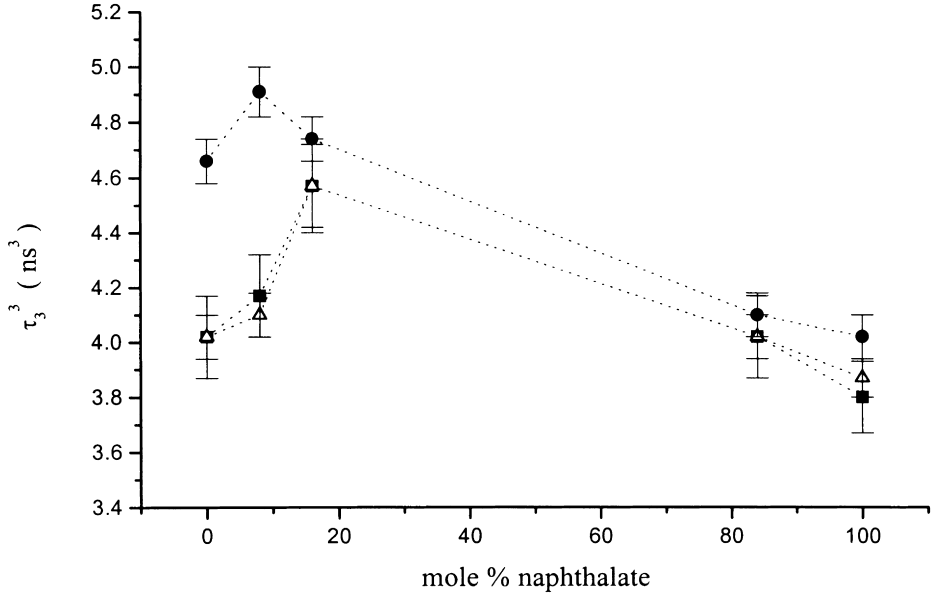

Fig. 2. τ_3^3 versus mol% naphthalate for (■) cast amorphous sheets, (●) low draw area and (△) high draw area biaxially oriented films.

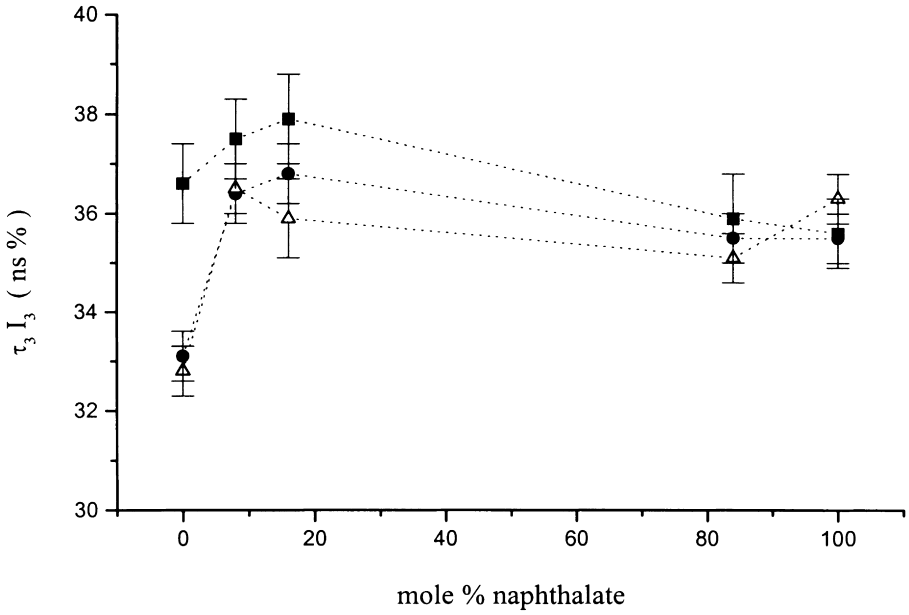

Fig. 3. $\tau_3 I_3$ versus mol% naphthalate for (□) cast amorphous sheets, (●) low draw area and (△) high draw area biaxially oriented films.

near 90°C for samples drawn at 87°C and attributed this 'endothermic' DSC peak to an amorphous to crystalline transformation of the *trans* isomers that are dispersed in the amorphous phase. Cakmak et al. [46] also observed a relaxation peak in the temperature range 100–140°C which they classified as being an 'exothermic' transition. Nevertheless, the origin of this chain relaxation peak is a consequence of the stretching process, and was inherent in all of the samples used in this study.

Incorporation of low levels of naphthalate caused a reduction in X_ρ relative to PET, due to the presence of the 'randomly' distributed naphthalate segments in the chain decreasing the efficiency of the alignment of PET segments. Greatly reduced values of X_ρ were measured for PETN84, PEN and the blend. The low values of X_ρ for the blend would be consistent with a greater number and distribution of environments in the system. As with the heat of fusion data, the density data failed to show significant differences between the low and high draw areas (Table 3). These observations are not unusual; indeed previous studies at

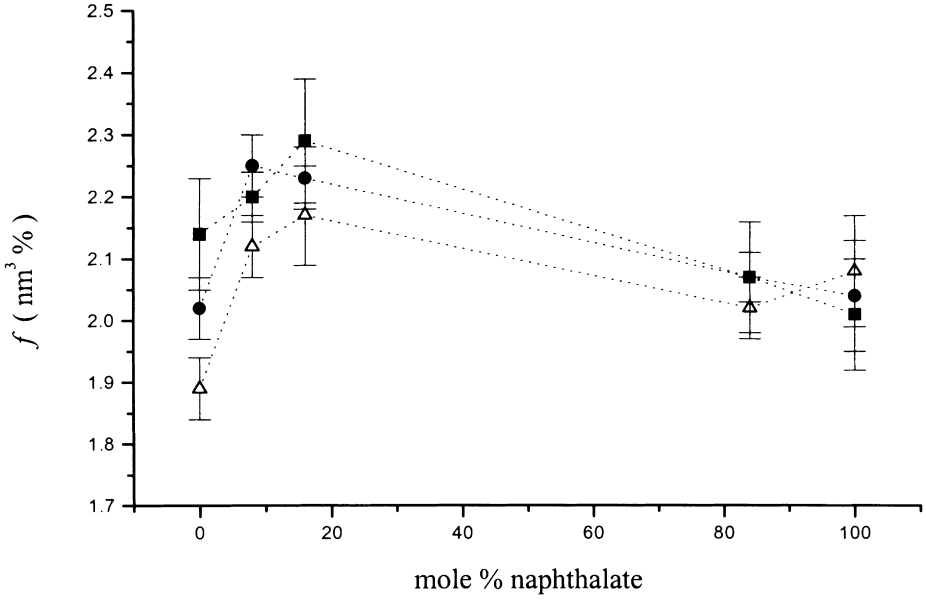

Fig. 4. Fractional free volume, *f*, versus mol% naphthalate for (■) cast amorphous sheets, (●) low draw area and (△) high draw area biaxially oriented films.

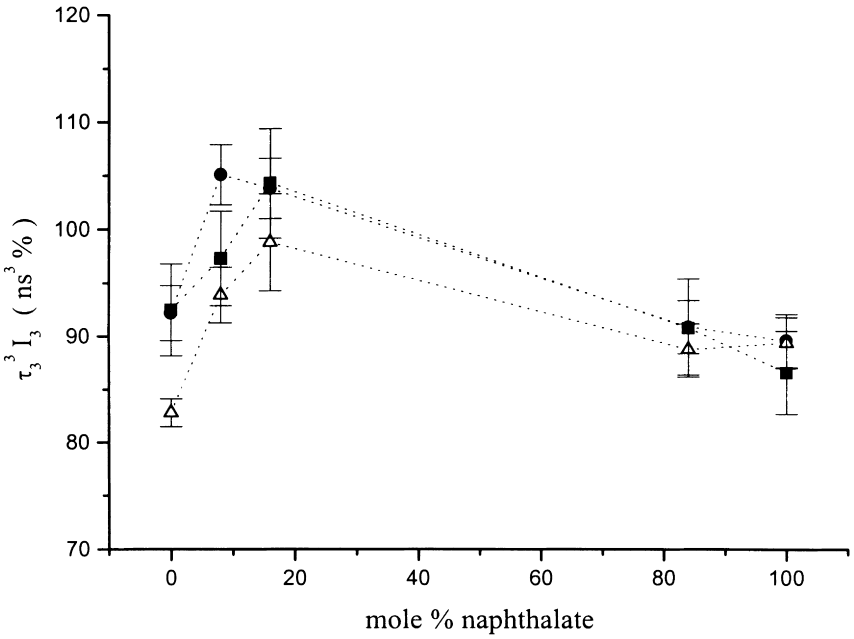

Fig. 5. $\tau_3^3 I_3$ versus mol% naphthalate for (■) cast amorphous sheets, (●) low draw area and (△) high draw area biaxially oriented films.

ICI Wilton on samples stretched at $T_g \pm 20$°C have shown similar trends with the degree of crystallinity reaching a 'plateau' value. In most instances X_ρ decreased slightly as the draw ratio was increased, except in the case of PETN16 and PETN84, where a small increase was observed.

4.2. Gas permeability

It is well known that glassy polymers exhibit more complex equilibrium sorption and transport behaviour than rubbery polymers [7,13]. When a polymer is exposed to a vapour, the gas molecules may dissolve in the matrix and change the microstructure. This dissolution process could lead to a reduction in the T_g and an increase in the specific volume. It is also possible in extreme cases that if the gas pressure is sufficiently high, the polymer matrix may become compressed and cause the T_g to increase and specific volume to decrease. There are a variety of different models implemented to describe the sorption and permeation of gases in glassy polymers (dual-mode model, a dual-mode partial-immobilisation model and a gas-polymer matrix model to name but a few).

Examination of the CO_2 transport data (Table 5) seems to suggest the possible need for the use of the 'dual-mode type' model, where the solubility of the penetrant molecules is described by both Henry's Law and Langmuir terms. To establish whether or not a dual-mode model was applicable in these polymers, the transport properties of PET, PETN8 and PEN at the low draw area were measured at pressures between 1 and 4 atm [47]. For PET and PEN, both P and K were observed to decrease with increasing CO_2 pressure, as expected for dual-mode transport. The diffusion coefficient remained virtually constant. A similar situation with P and K was found with the PETN8 copolymer, but this time D increased slightly as the pressure increased.

In a study of CO_2 and CH_4 transport in glassy aromatic polyesters Sheu et al. [48] also observed a decrease in permeability with gas pressure. A dual-mode transport model was used to allow for the contributions of microvoids present in the glassy polymers. They satisfactorily fitted CO_2 transport results (effectively D and K) in random and oriented samples of PET and PEN to both a dual mode and a gas-polymer matrix model. Although the former model gave a better fit to the experimental data, implications from additional experiments were that CO_2 interacted with the polymer and hence rendered the latter model more appropriate. Similarly, Brolly et al. have demonstrated that although the dual-mode model provided a slightly better fit to their data on the permeation of CO_2 through PET, the simple gas-polymer matrix model was adequate at low to moderate pressures [42].

In contrast with the dual-mode model, the gas-polymer matrix model assumes that only one population of penetrant exists, but does propose that there is an interaction between the penetrant and polymer matrix. Pace and Datyner [49] suggest that the gas transport process occurs by a combination of diffusion along the direction of oriented chains and jumps between the channels. The jumps between channels control the large-scale transport. In the gas-polymer matrix model, interactions between the penetrant and the polymer are thought to facilitate these jumps. Indeed, Brolly et al. found that exposure of PET to CO_2 increased the rate of co-operative main-chain motions; the rate increasing with increasing penetrant concentration [42]. Consequently, it may be concluded that that the simple time-lag experimental technique, based as it is upon the gas-polymer matrix model,

Table 9
Parameters calculated from raw PALS data for the cast amorphous and biaxially oriented films for gas transport correlation purposes

Sample	Draw area	$\tau_3 I_3$ (ns %)	τ_3^3 (ns^3)	f (nm^3 %)	$\tau_3^3 I_3$ (ns^3 %)
Laser +	CA	36.6 ± 0.8	4.02 ± 0.15	2.14 ± 0.09	92.5 ± 4.3
	6.8	33.1 ± 0.5	4.68 ± 0.08	2.02 ± 0.05	92.9 ± 2.6
	12.8	32.8 ± 0.5	4.02 ± 0.08	1.89 ± 0.05	82.8 ± 1.3
PETN8	CA	37.5 ± 0.8	4.17 ± 0.15	2.20 ± 0.04	97.3 ± 4.4
	6.8	36.4 ± 0.6	4.91 ± 0.09	2.25 ± 0.05	105.1 ± 2.8
	12.2	36.5 ± 0.5	4.10 ± 0.08	2.12 ± 0.05	93.4 ± 2.6
PETN16	CA	37.9 ± 0.9	4.57 ± 0.17	2.29 ± 0.10	104.3 ± 5.1
	7.0	36.8 ± 0.6	4.74 ± 0.08	2.23 ± 0.05	103.8 ± 2.8
	13.6	35.9 ± 0.8	4.57 ± 0.17	2.17 ± 0.08	98.8 ± 4.5
PETN84	CA	35.9 ± 0.9	4.02 ± 0.15	2.07 ± 0.04	90.9 ± 4.6
	10.5	35.5 ± 0.5	4.10 ± 0.08	2.07 ± 0.09	90.9 ± 2.5
	12.0	35.1 ± 0.5	4.02 ± 0.08	2.02 ± 0.05	88.8 ± 2.4
PEN	CA	35.6 ± 0.7	3.80 ± 0.13	2.02 ± 0.09	86.6 ± 3.9
	8.4	35.5 ± 0.5	4.02 ± 0.08	2.04 ± 0.09	89.6 ± 2.5
	12.2	36.3 ± 0.5	3.87 ± 0.07	2.08 ± 0.09	89.4 ± 2.4
BLEND	CA	35.7 ± 0.9	4.66 ± 0.17	2.18 ± 0.09	99.7 ± 4.9
	10.1	35.8 ± 0.5	4.41 ± 0.08	2.16 ± 0.05	96.2 ± 2.6
	14.7	35.3 ± 0.5	4.41 ± 0.08	2.10 ± 0.05	94.8 ± 2.6

remains a practical tool for the evaluation of the transport of CO_2 through PET.

4.3. PALS

Previous PALS studies on crystallinity effects have demonstrated that while τ_3 remains constant, I_3 decreases as crystallinity increases [26]. This suggests that most of the *o*-Ps pick-off annihilation occurs in the amorphous regions or at amorphous/crystalline interfaces and it has been shown that when the essentially amorphous cast films were stretched, crystallinity contents increased due to stress induced crystallisation. For PET and the low naphthalate PETN copolymers the crystallinity content was in the range 17–25% (by volume); whereas for the high naphthalate PETN copolymers, PEN and the blend, the crystalline content was reduced to 10% or lower. Generally speaking there was no increase in crystallinity on going from the low to high draw area films. Furthermore, the gas permeability results showed that stretching reduces *D* and tended to also increase the solubility component, a sensitive indicator of amorphous content. Additionally, the different gas molecules investigated proved to be effective probes of size for the void structure in polymer films.

It was found that relative to PET and PEN, copolymerisation or blending disrupted chain packing, reflected in an increase in PALS parameters (see Table 9). For PEN and the high PETN copolymers, lower PALS parameters were observed, reflecting a tendency to form densely packed structures.

The first parameter to be discussed will be V_F which through Eqs. (3) and (4) is a direct function of τ_3^3, data for which is shown in Fig. 2. The data for the low draw area naphthalate systems indicates that there is an increase in the cavity volume that decreases upon further stretching to a size more comparable with those observed in the cast amorphous films. Larger cavity sizes were measured for the blend in relation to PET and PEN and stretching did not cause major changes to the hole size. These changes in cavity size do not correlate with the measured gas diffusivity.

PALS parameters sensitive to hole size alone cannot adequately describe the morphological details of these systems. A better indication of the changes occurring can be obtained by calculating the product of $\tau_3 I_3$ which is a measure of the total void content. This highlighted a progressive decrease on going from cast amorphous film to low draw area and then high draw area film in PET, PETN8 and PETN16 (Fig. 3). A very slight increase in $\tau_3 I_3$ was observed for PEN at the high draw area, whereas the values were virtually constant for PETN84 and the blend.

An alternative way of assessing the effective void content is to calculate the fractional free volume, f (cf. Eq. (5)). The average gas diffusivity provides a measure of the effective mobility of the penetrant in the polymer matrix. If the gas molecule is comparable in size to the available hole size in the material, its diffusion will be restricted. However, if the gas molecule is smaller than the statistical average free volume, it will diffuse through the material with a large diffusion coefficient. The variation of f with naphthalate content is highlighted in Fig. 4, and clearly demonstrates the combined effects of polymer structure and processing on the calculated values. As before, a local minimum in packing density at the low naphthalate contents resulted in an

increase in f and appears to be in contradiction with the observed reduction in gas diffusivity in these systems. The progressive reduction in f for PET with stretching in contrast with the relatively constant f for PEN (and PETN84) parallels the observed gas diffusion behaviour.

As has been previously proposed [26], the parameter $\tau_3^3 I_3$ provides the best description of the free volume characteristics in these polyester systems. Because of the relationship between τ_3^3 and V_F, the overall trends are similar to those described for f. For PET, PETN16, PETN84 and the blend, $\tau_3^3 I_3$ decreased on stretching but an increase was noted on going from the cast film to the low draw area for PETN8 and PEN. A higher value is not unreasonable if one considers that the drawing process is likely to *disorganise* the chains before they become more densely packed [50]. With the exception of PEN, stretching to the higher draw area then caused the $\tau_3^3 I_3$ value to be reduced again relative to the cast film.

Whereas for polyimides [19] and polycarbonates [25] the hole radii, volumes, and fractions have a direct correlation with gas diffusion coefficients, this study has shown that this was not necessarily true for the polyesters and a larger hole size and fraction of free volume hole did not result in a higher gas diffusion rate. Recently, Xu et al. [51] acknowledged that free volume approaches for modelling gas transport still have room for improvement and, indeed, for the systems in this study the application of the correlations favoured by Hill et al. [26], Tanaka et al. [19] and Jean et al. [25] could not be successfully applied.

Both PET and PEN have sufficiently high glass transition temperatures, fast crystallisation rates and, therefore, the tendency to form compact, ordered structures with low free volumes. Therefore, it is perhaps not surprising that PALS did not determine large differences in free volume and free volume distribution between the homopolymers. In order for a free volume based theory of penetrant diffusion to be implemented, such as that based on the original work of Cohen and Turnbull [31], a linear relationship between the measured free volume and gas permeability (diffusivity) has to exist. However, such a relationship clearly does not exist for these systems. In fact it was observed that free volume increased for the copolymers and we attributed this to the chains attaining a more random nature, and thus hindering efficient packing.

5. Conclusions

The PALS experiments have shown that rather than static theories like free volume being used as the main explanation for differences in gas transport in these PET, PETN and PEN systems, dynamic theories such as those proposed by Light and Seymour [15] may be more appropriate. These polymers exhibit to a greater or lesser extent microcrystalline organisation and, therefore, a percolation element to the diffusion process would be expected. The data presented here indicates that whilst changes in the void size of the amorphous phase do occur with change in chemical structure and processing, it is probably the orientation and distribution of crystallites that plays a dominant role in determining the gas permeation behaviour.

Acknowledgements

The authors thank ICI Polyester (now Du Pont) and the EPSRC for funding the work. Special thanks to Paul Davis (Du Pont Polyester) for preparing the amorphous PET samples, performing the density measurements and oxygen permeability measurements.

References

[1] Ha H, Harrison IR. J Polym Sci, Polym Phys Ed 1992;30:915.
[2] Michaels AS, Bixler HJ. J Polym Sci 1961;50:393–413.
[3] Gohil RM, Salem D. J Appl Polym Sci 1993;47:1989.
[4] Gohil RM. J Appl Polym Sci 1993;48:1635.
[5] Chang H, Schultz JM, Gohil RM. J Macromol Sci Phys B 1993;32:99.
[6] Gohil RM. J Appl Polym Sci 1993;48:1649.
[7] Vieth WR. Diffusion in and through polymers: principles and applications. Munich: Hanser, 1990.
[8] Cakmak M, Kim JC. J Appl Polym Sci 1997;64:729.
[9] Kim JC, Cakmak M, Zhou X. Polymer 1998;39:4225.
[10] Cakmak M, Kim JC. J Appl Polym Sci 1997;65:2059.
[11] Murakami S, Nishikawa Y, Tsuji M, Kawaguchi A, Kohjiya S, Cakmak M. Polymer 1995;36:291.
[12] Heffelfinger CJ, Schmidt PG. J Appl Polym Sci 1965;9:2661.
[13] Naylor TdeV. Permeation properties. In: Allen G, Bevington JC, editors. Comprehensive polymer science, vol 2. Oxford: Pergamon Press, 1989.
[14] Young RJ, Lovell PA. Introduction to polymers. 2nd ed. London: Chapman and Hall, 1991.
[15] Light RR, Seymour RW. Polym Engng Sci 1982;22:857.
[16] Weinkauf DH, Paul DR. J Polym Sci, Polym Chem Ed 1992;30:817 (see also p. 837).
[17] Kim CK, Aguilar-Vega M, Paul DR. J Polym Sci, Polym Phys Ed 1992;30:1131.
[18] McGonigle E-A, Jenkins SD, Liggat JJ, Pethrick RA. Polym Int 2000 (in press).
[19] Tanaka K, Katsube M, Okamoto K, Kita H, Sueoka O, Ito Y. Bull Chem Soc Jpn 1992;65:1891.
[20] Haraya K, Hwang ST. J Membr Sci 1992;71:13.
[21] Nakanishi H, Jean YC. Macromolecules 1991;24:6618.
[22] Deng Q, Zandiehnadem H, Jean YC. Macromolecules 1992;25:1090.
[23] Deng Q, Jean YC. Macromolecules 1993;26:30.
[24] Kobayashi Y, Haraya K, Hattori S, Sasuga T. Polymer 1994;35:925.
[25] Jean YC, Yuan J-P, Liu J, Deng Q, Yang. J Polym Sci, Polym Phys Ed 1995;33:2365.
[26] Hill AJ, Weinhold S, Stack GM, Tant MR. Eur Polym J 1996;32:843.
[27] Hong X, Jean YC, Yang H, Jordan SS, Koros WJ. Macromolecules 1996;29:7859.
[28] Tao SJ. J Chem Phys 1972;56:5499.
[29] Eldrup M, Lightbody D, Sherwood JN. Chem Phys 1981;63:51.
[30] Nakanishi H, Wong SJ, Jean YC. In: Sharma SC, editor. Positron annihilation studies of fluids. Singapore: World Science, 1988.
[31] Cohen MH, Turnbull D. J Chem Phys 1959;31:1164.
[32] Paper in preparation.
[33] T.M. Long Co., Film Stretcher Instruction Manual, Somerville, NJ.
[34] Richardson MJ. Thermal analysis. In: Allen G, Bevington JC, editors. Comprehensive polymer science, vol 1. Oxford: Pergamon Press, 1989.

[35] Barrer RM. Diffusion in and through solids. Cambridge: Cambridge University Press, 1941.
[36] Davies WJ, Pethrick RA. Eur Polym J 1994;30:1289.
[37] Kirkegaard P, Pedersen NJ, Eldrup M. Patfit-88: a data processing system for positron annihilation spectra on mainframe and personal computers, Riso National Laboratory, Denmark, 1989.
[38] Groeninckx G, Reynaers H, Berghmans H, Smets G. J Polym Sci, Polym Phys Ed 1980;18:1131.
[39] Cheng SZD, Wunderlich B. Macromolecules 1988;21:789.
[40] Bouquerel F, Bourgin P, Perez J. Polymer 1992;33:516.
[41] Holden PS, Orchard GAJ, Ward IM. J Polym Sci, Phys Ed 1985;23:709.
[42] Brolly JB, Bower DI, Ward IM. J Polym Sci, Polym Phys Ed 1996;34:769.
[43] Pethrick RA. Prog Polym Sci 1997;22:1.
[44] Lu X, Windle AH. Polymer 1995;36:451.
[45] Cakmak M, White JL, Spruiell JE. J Polym Eng 1986;6:291.
[46] Lee KH, Sung CSP. Macromolecules 1993;26:3289.
[47] McGonigle E-A. PhD Thesis, University of Strathclyde, Glasgow, 1998.
[48] Sheu FR, Chern RT, Stannett VT, Hopfenberg HB. J Polym Sci, Polym Phys Ed 1988;26:883.
[49] Pace RJ, Datyner A. J Polym Sci, Polym Phys Ed 1979;17:437.
[50] Ward IM. Structure and properties of oriented polymers. London: Applied Science Publishers Ltd, 1975.
[51] Xu ZK, Böhning M, Springer J, Glatz FP, Mölhaupt R. J Polym Sci, Polym Phys Ed 1997;35:1855.